The Holocene 16,3 (2006) pp. 445–455

Holocene river floods in the upper Glomma catchment, southern Norway: a high-resolution multiproxy record from lacustrine sediments

Anne-Grete Bøe,[1,2*] Svein Olaf Dahl,[2,1] Øyvind Lie[1] and Atle Nesje[3,1]

([1]Bjerknes Centre for Climate Research, Allégaten 55, N-5007 Bergen, Norway; [2]Department of Geography, University of Bergen, Fosswinckelsgate 6, N-5007 Bergen, Norway; [3]Department of Earth Science, University of Bergen, Allégaten 41, N-5007 Bergen, Norway)

Received 1 June 2005; revised manuscript accepted 8 November 2005

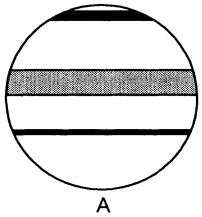

A HOLOCENE RESEARCH PAPER

Abstract: The Glomma catchment in east-central southern Norway has a discharge dominated by a general spring-flood regime with episodic large river floods. In this study, the instrumental records (from AD 1871) and documentary evidence (back to the seventeenth century) have been extended for about 10 000 years by reconstructing episodes of palaeofloods as recorded by sedimentological depositional indicators. A record of Holocene flood events has been established based on a lake-fill sedimentary succession in a small basin in the upper Glomma catchment. The flood events as deposited in Lake Butjønna are discrete, sharp-bounded, normal graded units of silt-sized sediments characterized by low organic and water content. The reconstruction of individual palaeofloods is based on loss-on-ignition, dry bulk density, grain-size analyses and several mineral magnetic analyses: initial susceptibility, bulk susceptibility (χ), anhysteretic remanent magnetization (ARM) and isothermal remanent magnetization (IRM). Based on 13 ^{14}C AMS dates, the age–depth model covers the Holocene from *c.* 9800 cal. yr BP until present. About 115 discrete flood events (ranging from 1 to 620 mm in thickness) have been detected. The recurrence interval is about 90 years with an occurrence probability of about 1%. Important results include: (1) a weak increasing trend of higher river flood activity toward the end of the Holocene; (2) an early-Holocene calm (low or no river flood activity) period with subsequent onset of flood activity around 7600 cal. yr BP; (3) a pronounced and well-defined river flood event correlated to the 'Stor-Ofsen' disaster that occurred in July AD 1789; (4) enhanced southerly winds that bring moist air from the Atlantic Ocean apparently lead to periods of higher river flood frequency.

Key words: River floods, Holocene palaeoflood record, lacustrine sediments, environmental magnetism, southern Norway.

Introduction

There has been increased focus during the last few decades on the emerging evidence regarding the higher frequency of severe floods during the twentieth century (eg, Milly *et al.*, 2002; Benito, 2003; Bronstert, 2003; Macklin and Lewin, 2003; Mudelsee *et al.*, 2003). River floods are among the most common and widespread of all natural hazards and Holocene fluvial sedimentary records seem to reflect global climate changes (Starkel, 2002; Macklin and Lewin, 2003; Thorndycraft *et al.*, 2003). The degree to which flood disasters and clustering are related to an enhanced greenhouse warming is a matter of ongoing debate (Christensen and Christensen, 2002; Brazdil *et al.*, 2002; Lins and Cohn, 2003; Mudelsee *et al.*, 2003). There are several climatic settings that may trigger flood events in small systems, such as excessive rainfall, snowmelt or rain-on-snow events. Hence, changes in the amount, frequency and intensity of precipitation have an effect on snow storage, the magnitude and timing of runoff, and thereby flood occurrence and intensity. Recent investigations of different archives have shown several millennial-scale climatic events

*Author for correspondence (e-mail: anne-grete.boe@bjerknes.uib.no)

10.1191/0959683606hl940rp

throughout the Holocene (eg, Bond *et al.*, 1997; Seppä and Birks, 2001; Briffa *et al.*, 2004). Lake sediment records of river floods provide a proxy archive of environmental history at the event scale, and it has been shown that changes in flood characteristics have occurred abruptly at various timescales (Bronstert, 2003). These changes may result from variations in circulation patterns, storm tracks and air-mass boundaries (Knox, 2000).

In Norway, the main rivers that constitute the approximately 41 000 km^2 Glomma catchment, the country's largest, have been studied in detail using historical incidents (eg, Østmoe, 1985; Roald, 1999, 2003), sediment transport (Bogen, 1989, 2004; Tvede, 2004) and modern flooding and continuous surveillance and management by the Norwegian Water and Energy Directorate (NVE). Flooding resulting from snowmelt and possible simultaneous rainfall are of primary concern in eastern Norway, as all river Glomma floods exceeding 2000 m^3/s have happened during May–June. Gauge measurements (NVE) at Elverum covering the timespan 1871–2003 (AD 1995 shown in Figure 1), reveal several megafloods in AD 1934 (2962 m^3/s), 1916 (2892 m^3/s), 1890 (2360 m^3/s), 1887 (2354 m^3/s) and 1879 (2296 m^3/s). Studies on suggested extreme climate/weather-induced slope processes in southern Norway include investigations of scree material (Blikra and Nesje, 1997; Blikra and Fjellstad Selvik, 1998; Blikra and Nemec, 1998), debris flows (Sletten *et al.*, 2003) and snow-avalanches (Seierstad *et al.*, 2002). A flood marker based on historical reports of the River Glomma at Elverum shows 20 damaging floods (Figure 1) ranked in order of decreasing size in AD 1789, 1995, 1773, 1675, 1717, 1724, 1749, 1827, 1934, 1850, 1916, 1846, 1760, 1966 and 1967 (Norges Offentlige Utredninger (NOU), 1996). The AD 1789 event, the most severe flood in Norwegian historical records, was caused by excessive rainfall on top of delayed snowmelt, culminating on 22 July (Sommerfeldt, 1943; Østmoe, 1985). Documentary evidence on palaeofloods consists primarily of systematic gauge measurements and non-systematic data from written reports and flood marks (Brazdil *et al.*, 2002). The history and development of flood frequency and magnitude in a river system beyond the historical record have been reconstructed from the sedimentary archive found in lake sediments (Thorndycraft *et al.*, 1998; Brown *et al.*, 2000, Nesje *et al.*, 2001a).

The objective of this study was to investigate the natural sediment archive present in a small basin in the upper Glomma catchment to look at proxy data for occurrence of flood events in an undisturbed long sediment succession. Flood-related discharges result in the deposition of laterally consistent horizons of silty sediments in Lake Butjønna. The sediment succession was used to generate a high-resolution ^{14}C-dated Holocene record. The flood record was then compared with reconstructed regional winter precipitation and debris flows from intensive rainstorms.

Study area and methods

The river Sagbekken drains a small ($\sim$15 km^2) and low-relief (altitude $\sim$670–1200 m) mountainous catchment into Lake Butjønna (667 m a.s.l.) in Folldal (Figure 2). The lake is dominated by autochthonous organic production and the surrounding vegetation consists of pine and birch forest, whereas mosses and lichens cover the terraces in the area. Colluvial disturbance of the lake sediments is considered unlikely, as the lake is located on a flat glaciofluvial terrace (Sollid and Carlson, 1979) about 1 km from the valley slope in a tectonically stable area. The climate is continental, with a mean (1961–1990) annual precipitation and temperature of 364 mm and 0.7°C, respectively, at Fokstua, 38 km from the study site (Det Norske Meteorologiske Institutt (DNMI), 1993). Approximately one-third of the annual precipitation falls as snow in the low-lying areas and relatively more with increasing altitude. Except for south-southeasterly winds, the area is in the rain shadow for prevailing winds from southwest, northwest and north.

Lake coring and sediment analyses

A bathymetric survey was carried out and revealed two basins in Lake Butjønna with a maximum water depth of about 10 m (Figure 2). Four cores (diameter 110 mm and up to 5.3 m long) were retrieved by a piston corer (Nesje, 1992) operated from a raft. All cores were stored in a cool (+4°C) and dark place.

Visual logs and photographs from all cores were taken before any further investigations. X-ray measurements and continuous surface core analyses by a non-destructive Multi Sensor Core Logger (MSCL) including γ-rays, magnetic susceptibility (10^{-5} SI) and density measurements (Gunn and Best, 1998) were performed at 0.2 cm intervals.

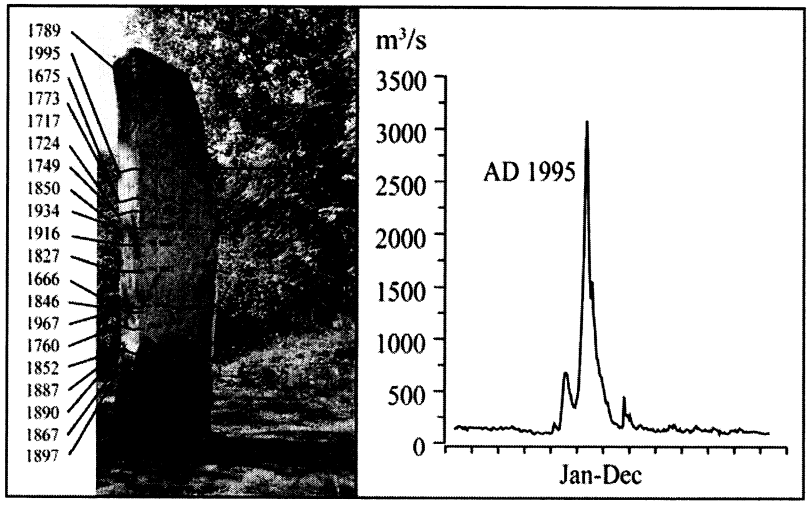

Figure 1 Left: a 3 m high historical flood marker at Elverum, downstream in the Glomma catchment in the valley Østerdalen. It shows the 19 largest floods over the last centuries and their ages. Right: daily gauge measurements (m^3/s from NVE) from the year of the second largest flood in this catchment, 'Vesle-Ofsen' AD 1995 at Elverum

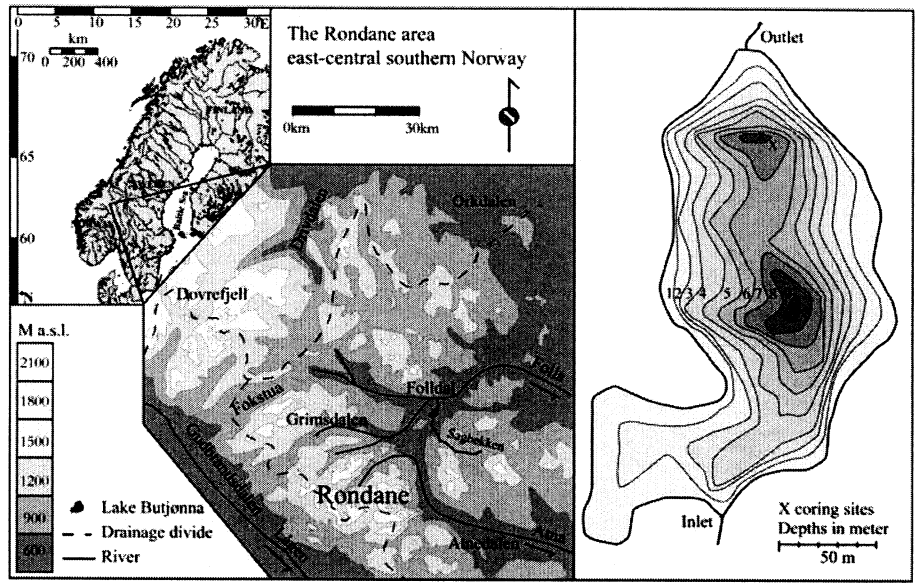

Figure 2 Left: location map of Lake Butjønna, 667 m a.s.l. 62°08′ N 10°10′ E, in the upper Glomma catchment, east-central southern Norway. Right: bathymetric map of Lake Butjønna with 1 m contour lines. The two deepest troughs were preferred coring sites

Twelve terrestrial plant macrofossils were extracted and identified for accelerator mass spectrometry (AMS) ^{14}C-dating at the Poznan Radiocarbon Laboratory in Poland, while five bulk samples and one macrofossil sample were processed at Trondheim Radiological Laboratory in Norway (Table 1). Wet and dry bulk density (dried overnight at 105°C), loss-on-ignition (LOI, 1 h at 550°C) and grain-size analysis (0.1 and 300 μm) by a Micromeritics SediGraph 5100 were carried out at 1-cm contiguous samples. Carbonate content was inferred from LOI at 950°C measured at 5 cm intervals.

Mineral magnetic analyses were executed at 1-cm sampling intervals with 2 × 2 × 2 cm plastic boxes: bulk susceptibility (MS, χbulk), anhysteretic remanent magnetization (ARM, χARM) and isothermal remanent magnetization (IRM, σIRM). Acronyms of magnetic parameters used in this paper follow the procedures of Walden *et al.* (1997, Appendix 1). χbulk values were initially determined on both wet and freeze-dried samples on a KLY-2 induction bridge (sensitivity: 4×10^{-8} SI).

χARM was obtained by arranging a 0.1 mT DC field and a 100 mT AC field in a 2G afdemagnetizer. Low field mass-specific susceptibility is nearly independent of grain-size within the single domain (SD, 0.03–0.05 μm) to multidomain (MD, > 10 μm) region and SD appears only slightly lower than MD. SD grains have high intensity per unit mass, which makes χARM a proxy for SD. σIRM was measured on either a Digico spinner (noise level 5×10^{-7} A/m) or a three-axis Cryogenic magnetometer (CCL 350/450; noise level 3×10^{-8} A/m). S-ratio ($\sigma IRM_{-0.1T \text{ or } -0.3T}/\sigma SIRM_{3T}$) gives additional information about mineralogical composition (Evans and Heller, 2001; Paasche *et al.*, 2004). Variations in concentration and magnetic grain-size are reflected in the relationship χARM/χbulk. Bacterial magnetite (*Magnetospirillum magnetotacticum*) produces SD-magnetite, acknowledged by σARM/σSIRM ratios > 0.1 (eg, Paasche *et al.*, 2004).

Table 1 AMS ^{14}C ages derived from macrofossil and bulk samples, from Lake Butjønna

Core	Depth (cm)	Laboratory no.	Sample material	Dates ^{14}C yr BP	Calibrated ages[a] (cal. yr BP) (Intcal98/Calib rev 4.4)
03butj3	66	Historical data	Sedimentological transition		161
03butj3	66	Poz-4770	*Betula* sp., twig	170±25	145±145
03butj3	67	Poz-4791	*Betula* sp., leaf	200±30	152±150
03butj3	105	Poz-4792	*Pinus sylvestris*, bark	545±30	574±60
03butj3	147	Poz-4772	*Pinus sylvestris*, needle	1315±30	1235±55
03butj3	214	Poz-4773	*Betula* sp., leaf	2060±30	2032±84
03butj3	248	Poz-4774	*Betula* sp., leaf	2685±30	2799±47
03butj3	313	Poz-4775	*Betula* sp., twig	3565±30	3844±119
03butj3	399	Poz-4776	*Pinus sylvestris*, bark	5265±35	6051±119
03butj3	424	Poz-4793	*Betula* sp., leaf	6020±40	6853±119
03butj3	448	Poz-4777	*Pinus sylvestris*, needle	6750±40	7593±80
03butj3	504	Poz-4778	*Betula* sp., twig	8220±40	9214±184
03butj3	528	Poz-4794	*Betula* sp., leaf	8530±50	9514±83
00butj2	119	T-15453A	Bulk	820±85	789±136
00butj2	208	T-15451A	Bulk	2980±85	3152±207
00butj2	407	T-15450A	Bulk	4340±100	5050±244
00butj2	492	TUa-3210	Bulk	7480±80	8284±125
00butj2	518		Bulk		8190±100
00butj2	530	T-15449A	*Pinus sylvestris*, bark	8720±160	9837±347

[a]Calibrated ages (cal. yr BP) from Intcal98/Calib rev 4.4 (Stuiver *et al.*, 1998).

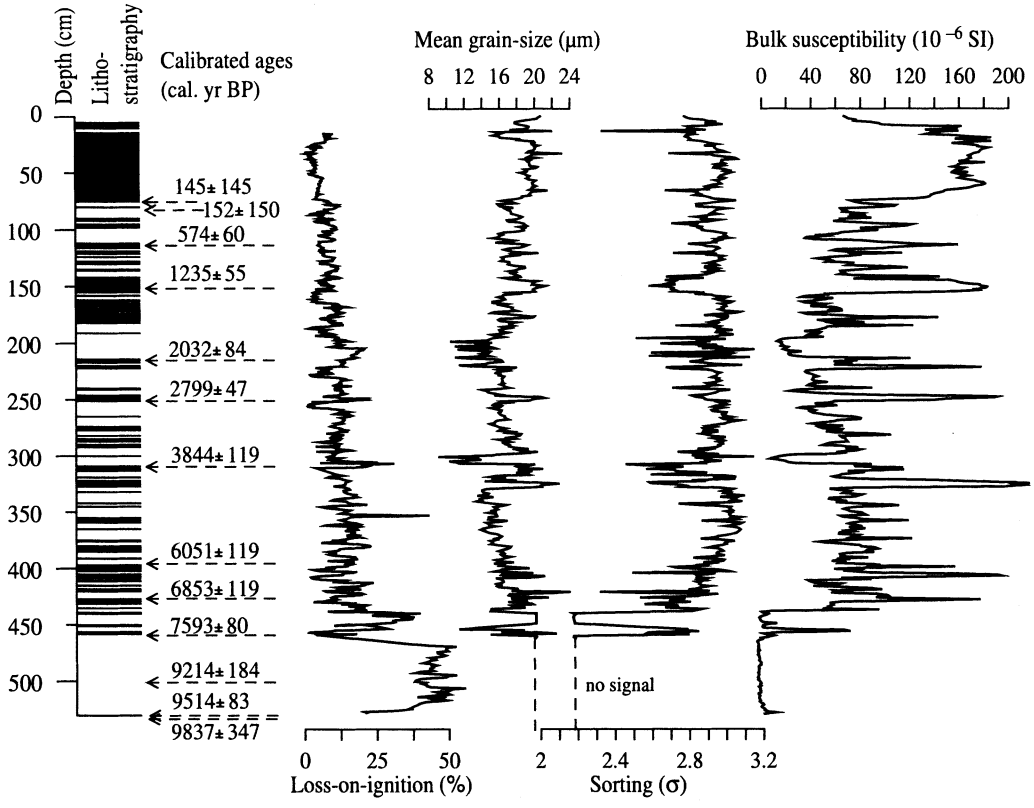

Figure 3 The master core from Lake Butjønna. The data include radiocarbon dates, visual logging (also from X-ray imaging), lithostratigraphy (floods represented with a black bar), loss-on-ignition, mean grain-size, sorting and initial magnetic susceptibility

Results

A general lithostratigraphy based on visual logging, LOI and MSCL profiles is presented in Figure 3. Grain-size data derived from X-ray analysis are discussed with special emphasis on mean, sorting and skewness. Variations in environmental magnetism generate further stratigraphical subdivision.

Lithostratigraphy

Two main lithostratigraphic units (type A and B) are recognized in all cores based on visual logging, X-ray measurements, MSCL and LOI data (Figure 3). Type A consists of organic brown or black coloured layered gyttja. The LOI values are high (average 43.2%) with corresponding low values of magnetic susceptibility (average $\sim 10 \times 10^{-6}$ SI). The magnetic susceptibility and LOI values are negatively correlated ($r = -0.79$). Type B consists of light grey, low-organic silty or sandy laminae or layers (1–620 mm in thickness) with high values of magnetic susceptibility (average $\sim 30 \times 10^{-6}$ SI) and low (3.1–10.5%) LOI values.

Type A is associated with hydrologically stable periods characterized by no or low-magnitude river flood activity. The brown or black coloured organic material comes from both the lake catchment (allochthonous) and organic material produced in the lake (autochthonous) (eg, Bogen, 1983). Type B is irregularly distributed and is associated with episodes/periods of higher sedimentation energy.

Loss-on-ignition and grain-size distribution

Overall (both type A and B) LOI values vary considerably with an average of 36.4% (Figure 3). Taking into account only samples containing minerogenic type B units, the LOI values vary from 3.1 to 10.5%, depending on the thickness of the unit. The type B grain sizes are values commonly between 10.9 and 23.1 μm (medium to very coarse silt). The minerogenic horizons also contain a considerable amount of plant remains, as described and recognized in turbid deposits in lacustrine sediments (Sletten *et al.*, 2003).

The whole sequence reveals negatively skewed grain-size distributions, which implies an excess of fine particles relative to the mean and median. The mean grain-size value is low, but tends to have a fine tail that may indicate both enhanced competence (increased grain-size) and capacity (finer particles in suspension). The skewness and mean grain-size correlate well with a coefficient of determination of $R^2 = 0.98$ ($r = -0.99$). This suggests that larger grain-sizes are associated with enrichment of fine particles relative to the mean grain-size distribution because of an excess of fine particles in suspension during high-energy discharge.

As the sorting (σ_g) varies between 2.2 and 3.2 (Figure 4), all samples are defined as poorly sorted. There are no trends in the record pointing at wide-ranging changes in the water flow speed, but episodic changes in accordance with high minerogenic sedimentation are detected. Based on layer thickness, the minerogenic layers are divided into eight classes: 37 of 1 mm, 36 of 5 mm, 31 of 10 mm, 5 of 30 mm, 2 of 45 mm, 1 of 55 mm, 1 of 115 mm and 1 of 620 mm. Based on the average of all samples (1-cm contiguous intervals) of type B, the mean grain-size value increases with sediment layer thickness, and spans from 16.9 to 19.1 μm (Figure 4). The sorting shows an equivalent trend (2.3–2.9 σ_g), and the two values demonstrate a negative correlation, $r = -0.7$ (Figure 4). Type B are related to high mean grain-size and better sorting, which in turn is associated with increased runoff, higher competence and higher sediment influx.

A mean/sorting-ratio is established and plotted against each thickness class (Figure 4). No significant relationships have been observed between thickness, mean grain size and amount of accumulated organic material since last event. The grain size appears normally graded throughout a layer.

There is a positive relationship between mean grain size and very fine sand ($r = 0.87$) and very coarse silt ($r = 0.92$), and a

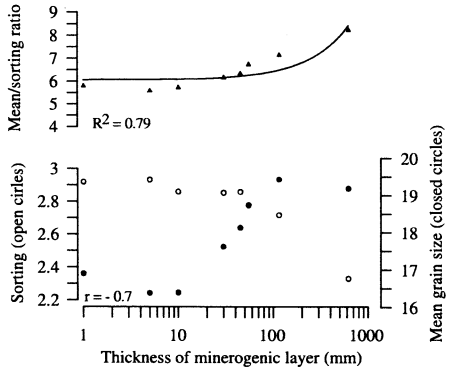

Figure 4 Correlation between mean grain-size and sorting in the thickness classes (mm): 1, 5, 10, 30, 45, 55, 105 and 620. Lower panel: sorting (open circles) and mean (solid circles) with a correlation coefficient, $r = -0.70$. Upper panel: mean/sorting-ratio with best (linear) curve fit ($Y = 0.00378 \times +6.05263$) with a coefficient of determination, $R^2 = 0.79$. Note the logarithmic (common) scaled x-axis

corresponding negative relationship to the finer grain sizes: very fine silt ($r = -0.90$) and clay (-0.82). There is no significant relationship between LOI and the different grain size fractions. LOI, however, changes significantly ($r = -0.79$) with bulk magnetic susceptibility (Figure 3).

A prominent type B unit of 620 mm (Figure 3), demonstrates a consequently negative relationship between the mean grain size (average of 19.2 μm, varies from 15.3 to 23.1 μm) and sorting (average of 2.9 σ_g varies from 2.3 to 3.1 σ_g). A strong positive correlation ($r = 0.90$) between very coarse silt and mean grain-size is found. The record shows three distinct incidents of higher mean grain-size values at 69, 36 and 16 cm. This coincides with better-sorted sediments and a higher proportion of very coarse silt. According to the ^{14}C dates (Table 1) and historical records (eg, Sommerfeldt, 1943; Østmoe, 1985; Roald, 2003), this event corresponds to a major eighteenth-century flood disaster: 'Stor-Ofsen' in July AD 1789.

Environmental magnetism

Visual interpretation and enviromagnetic investigations suggest five main sedimentary phases (I–V) based on trends and amplitude of initial susceptibility (χbulk). These subdivisions are based on the composition of magnetic minerals (S-ratio, σSIRM) and magnetic particle-size characteristics (χARM/χbulk and σARM/σSIRM).

Phase I (530–440 cm)

The mean χbulk value is 0.7×10^{-8} m³/kg, an order of ten less than in the succeeding phase II. There is a single peak at the bottom, congruent with a 10 mm type B unit. At 456 cm, the start of a 30 mm thick type B unit matches a triple-pulsed χbulk-signature with a maximum value of 5.2×10^{-8} m³/kg. Analogous units are reflected by χbulk values of $10–12 \times 10^{-8}$ m³/kg that indicate that this phase is nearly non-magnetic (Figure 5). The lack of σSIRM and PARM signals is a clear contrast to the up-core record.

Phase II (439–330 cm)

This phase has a stable χbulk signal with a mean of 7.1×10^{-8} m³/kg. The mineralogical composition inferred from the S-ratio ($\sigma IRM_{-0.1T}/\sigma SIRM_{3T}$) is defined by a gradual build-up and sudden termination of high values, and suggests a dominance of 'softer' S-ratios indicative of magnetite (Figure 5).

Phase III (329–197 cm)

Phase III displays gradual up-core deterioration in the χbulk signal, but contains three (at 329, 250 and 225 cm) peaks in all parameters (Figure 5). χARM shows small relative variations,

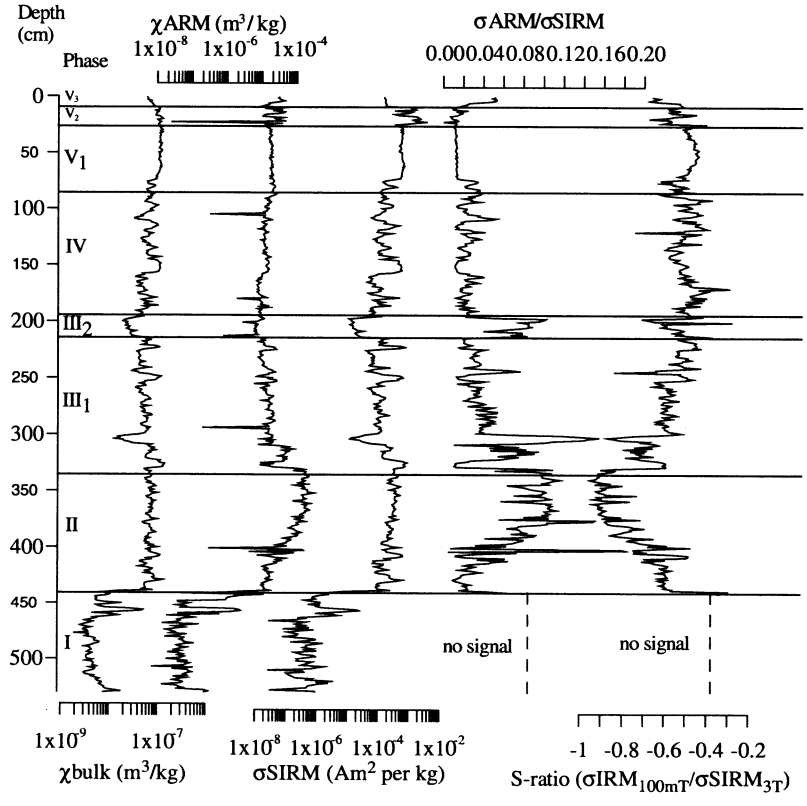

Figure 5 Magnetic concentrations (χbulk, χARM and σSIRM), mineralogy (S-ratio ($\sigma IRM_{-0.1T}/\sigma SIRM_{3T}$) and magnetic particle-size (PARM/PSIRM). The bulk susceptibility measurement in Figure 3 is averaged from a Gaussian detection curve (detection window of several centimetres) whereas here, magnetic measurements are carried out on boxes. This explains higher values and the occurrence of peaks

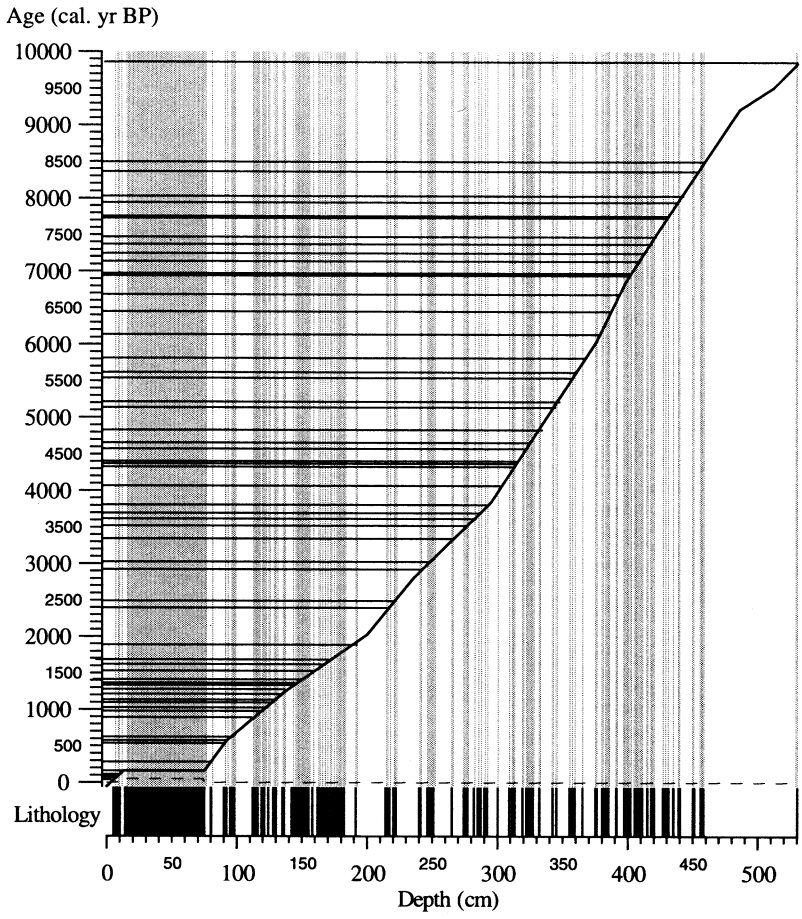

Figure 6 Age–depth model of core 00butj2 (coupled with 03butj3) based on AMS ^{14}C-dating of 13 plant macrofossil samples and one historical horizon (AD 1789). The curve is based on a linear regression model with two standard deviations. Lower bars show river flood occurrence

but σARM/σSIRM ratios >0.1 (214–197 cm) reflect the presence of magnetite (in SD or pseudo-single-domain (PSD) range) possibly caused by bacterial magnetite. The largest variances in the χbulk signal in combination with a well-defined rise in χARM occur in phase III_1.

Phase IV (196–76 cm)

High amplitude fluctuations in a rising trend of χbulk values with four large positive peaks $>10 \times 10^{-8}$ m^3/kg are detected. These peaks correspond to distinct incidents of higher σSIRM values, but with no χARM deflection.

Phase V (75–0 cm)

The concentration of magnetic material is relatively high ($10–12 \times 10^{-8}$ m^3/kg). Phase V_{1-2} equals the presented 620 mm thick type B unit (75–13 cm). Larger particle-sizes dominate the magnetic population of phase V_1 according to a positive shift exclusively in σSIRM ($\sim 60 \times 10^{-6}$ A/m) (Figure 5). In phase V_2, the concentration of magnetic minerals remains the same, and the occurrence of MD particles >10 μm is evident from the extreme σSIRM values (Figure 5). The PARM intensity shows small amplitude wiggling between $0–5 \times 10^{-5}$ Am^2/kg in phase V_{2-3}. Phase V_3 (12–0 cm) has a χbulk bulk susceptibility of $5–10 \times 10^{-8}$ m^3/kg with a few small fluctuations. Magnetic granolumetry (σARM/ σSIRM) is less dominated by large MD particles.

Chronostratigraphy

Two types of samples were ^{14}C dated and are stratigraphically consistent (Table 1): five bulk samples of gyttja and 13 samples of terrestrial plant macrofossils. However, only terrestrial plant macrofossils are used in the age–depth model (Figure 6). The sediments consist of fine-grained minerogenic layered units, and gyttja consisting of aquatic plant-remains and unevenly distributed terrestrial plant fragments. The LOI at 950°C shows inferred calcium carbonate ($CaCO_3$) values of less than 3.5%. The ^{14}C dates were calibrated by Calib (Intcal98) and Oxcal (Intcal98) (Stuiver *et al.*, 1998). The deviation between the two methods is negligible, and Calib (Intcal98) was employed. The 95.4% percentile intercept is used with two standard deviations. A coupled age–depth model was then established by a linear regression model after subtraction of the minerogenic horizons (Figure 6).

Discussion

Detection of Holocene river floods in lacustrine sediments

Minerogenic horizons are deposited irregularly and these discrete sharp-bounded clastic sediments are associated with surface soil erosion during individual river flooding events. Such delivery of allochtonous minerogenic material into lakes is also described by Thorndycraft *et al.* (1998) and Brown *et al.* (2000). Similar discontinuous minerogenic horizons in organic successions have moreover been interpreted as high-density turbidites attributed to subaerial debris flows plunging into a lake (Sletten *et al.*, 2003).

Flood deposits are fine-grained sediments that settle out of suspension from floodwaters. Other possible sources for such sediments are glacigenic (eg, Dahl *et al.*, 2003), colluvial or

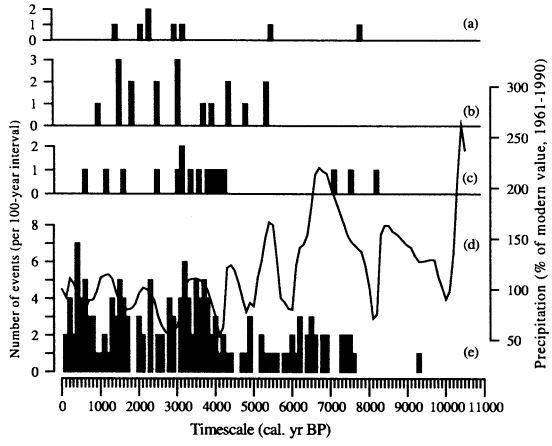

Figure 7 Compilation of recorded extreme weather events in southern Norway; Holocene colluvial and river flood activity. (a) Eight events recorded in Lake Ulvådalsvatnet, western Norway (Sletten *et al.*, 2003); (b) 18 debris-flow events elsewhere in western Norway (Blikra and Nesje, 1997; Matthews *et al.*, 1997); (c) 17 debris-flow events recorded at the Leirdalen site, eastern Norway (Matthews *et al.*, 1997), (e) 115 river flood events in Lake Butjønna, eastern Norway; and (d) reconstructed winter precipitation (percentage of 1961–90 values, solid line) from the plateau Glacier Hardangerjøkulen (Dahl and Nesje, 1996)

alluvial (eg, Blikra and Nemec, 1998). There is no glacier in the catchment, and the basin with its lake-fill sedimentary succession has been stable according to the following aspects: (1) the distinct type B units display normal grading without any erosional contacts, (2) sedimentation rate and accumulation suggest an invariable setting, and (3) there are no inverted ^{14}C-ages. The catchment and basin have not undergone any kind of modification as far as historical information is concerned, and human effects are negligible. Hence, enhanced discharge during river flooding is regarded as the most likely explanation for deposition of type B units in Lake Butjønna.

According to the linear regression model (Figure 6), the overall sedimentation rate is 0.48 mm/yr, which suggests a general time resolution of ~2 yr/cm. The sedimentation rate varies from 0.25 mm/yr (*c.* 6500–6000 cal. yr BP) to 0.77 mm/yr (*c.* 9800–9500 cal. yr BP) and allows a reconstruction of Holocene river flood frequency on a decadal timescale.

Utilization of sedimentological parameters

The negatively correlated LOI to magnetic susceptibility is fundamental to the general lithostratigraphy, which separates the normal organic accumulation (type A) from river flood episodes (type B). Larger grain-sizes in flood layers are also associated with enrichment of fine particles and a negative skewness relative to the grain-size distribution. This distributional skewness is the degree of asymmetry in the population. Fluvial sediments tend to be fine-skewed as a function of packing of fines in the sedimentary record, and deposition of the large grain-sizes allows smaller grains to settle between.

The mean grain size versus sorting is a useful energy indicator. The mean grain size is also vulnerable to the availability of sediments. Poor sorting is achievable in fluvial sediments that do not undergo extensive post-depositional reworking. Increasing unit thickness is associated with increasing mean grain size, which implies increased transport competence (Figure 4). This principle of corresponding energy correlation between sorting and the mean has been described by Arnaud *et al.* (2002) and Bakke *et al.* (2005).

The flood-layer thickness is expected to depend mainly on flood capacity and duration. Flood competence is, on the other hand, related to the maximum discharge rate. A study of the adjacent River Atna demonstrated a modern average erosion of 2.36 tons/yr per km^2 in the lower parts from sources of glacigenic origin (Bogen and Bønsnes, 1999). The ordinary sediment concentration (non-organic material in suspension) from May to November was less than 15 mg/L. In the AD 1995 flood, the flow discharge had to reach 600 m^3/s to increase the sediment concentration significantly (to 750 mg/L). The water level had to rise considerably to erode available deposits, and this explains why comparable energy levels result in different depositional units according to the timing and magnitude of previous flooding. The mean grain size is in Lake Butjønna are controlled by very fine sand ($r = 0.87$) and very coarse silt ($r = 0.92$), and a shortage of fines suggests that only floods of a given magnitude are identifiable in the Butjønna flood archive.

The 1-cm resolution (1 cm equals about 8 h) of the 620 mm thick type B unit allows detailed investigation of the flood disaster 'Stor-Ofsen' in AD 1789. During the approximately 20 days, escalated flood intensity occurred in three episodes. Coarse silt dominates the signal, which is in accordance with the assumed extreme magnitude of 'Stor-Ofsen'.

Magnetic phases

The nearly non-magnetic phase I (530–440 cm, ~10 500–7900 cal. yr BP) has two possible explanations. Either there was no river input at all, or the depositional regime experienced nearly no river flooding (calm period). The former view would have implied poor flood-archive validity for this period, but a flood layer at 518 cm (*c.* 9300 cal. yr BP) and no

Table 2 Recurrence interval (T) and flood occurrence probability ($P = 1/T$). Empirical mean (T_1 = number of flood in each thickness group/n) and statistical estimates ($T_2 = (n+1)/m$, $T_3 = 2n/(2m-1)$ and $T_4 = (\mathrm{m} - 0.44)/(n+0.12)$) calculated from different statistical weighing of the parameters: thickness, number of floods, rank and years of observation ($n \approx 9800$), m = rank number, largest observed flood = 1. T_4 is calculated using Gringorten's equation

Thickness (mm)	Number of floods	Rank	Recurrence interval (T) years				Probability (P)			
			T_1	T_2	T_3	T_4	P_1	P_2	P_3	P_4
1	37	8	250	1230	1310	1300	0.0041	0.0008	0.0007	0.0008
5	36	7	250	1400	1510	1500	0.0039	0.0007	0.0007	0.0007
10	31	6	390	1640	1790	1770	0.0025	0.0006	0.0006	0.0006
30	5	5	1970	1970	2180	2160	0.0005	0.0005	0.0005	0.0005
45	2	4	4920	2460	2810	2760	0.0002	0.0004	0.0004	0.0004
55	1	3	9840	3280	3940	3840	0.0001	0.0003	0.0003	0.0003
115	1	2	9840	4920	6560	6300	0.0001	0.0002	0.0002	0.0002
620	1	1	9840	9840	19 670	17 570	0.0001	0.0001	0.0001	0.00005
	114	Total	90				0.0116			

geomorphological evidence for river channel shifts eliminate this possibility.

Regarding different magnetic minerals, the S-ratio shows a gradual build-up and sudden termination of high (>0.1) values with a dominance of magnetite (Figure 5) in phase II (439–330 cm, *c.* 7900–4700 cal. yr BP). The σARM/σSIRM ratio-values >0.1 are accompanied by a colour change to brownish gyttja. The sudden termination at 330 cm is related to a 55 mm type B unit. Immediately after this flood event, the probable population of magnetic bacteria continued to live for some time (until 310 cm). However, a clear descending trend is shown and the bacterial magnetite apparently vanished entirely with a small (1-mm) flood at *c.* 4000 cal. yr BP in phase III (at 300 cm).

Any layer in phase III (329–197 cm, *c.* 4700–2100 cal. yr BP) with a χbulk susceptibility value above 9×10^{-8} m^3/kg is a flood event, according to the magnetic activity in the basin. The third and last period of σARM/ σSIRM ratio-values >0.1 and the possible presence of bacterial magnetite occurs at the end of phase III_2 (214–197, *c.* 2400–2000 cal. yr BP). A generally increasing trend with high-amplitude variation in the concentration of magnetic particles in phase IV (196–76 cm, *c.* 2100–161 cal. yr BP) was caused by increasing flood frequency. Stable composition of magnetic minerals expresses continuous source area.

Phase V (75–0 cm) covering the period 161–0 cal. yr BP is different from the rest of the core. χbulk susceptibility values ($10–12 \times 10^{-8}$ m^3/kg) reflect continuous high minerogenic input of larger MD magnetic grains (σSIRM values $\sim 60 \times 10^{-6}$ A/m). The extreme σSIRM values and occurrence of MD grains >10 μm in phase V_2 (30–12 cm) mirror the culmination of 'Stor-Ofsen' and show the possible import of particles from a broader source area. The nearby regional River Grimsa may have interfered with the drainage from the local River Sagbekken. The magnitude of this megaflood with raised water level impelled the larger adjacent River Grimsa to overflow its banks severely. In this case, a mixed sediment transport is a probable consequence. Deduced from the proportion of larger magnetic grains falling out of suspension, the erosion basis was higher, whereas the smaller fraction was carried further downstream.

Flood frequency

Several periods of enhanced river flood activity have occurred (Figure 7) and the Lake Butjønna archive experienced a trend of increased flood frequency towards the end of the Holocene. The flood frequency (number of floods per 100-yr interval) varies between zero (early Holocene) and seven (*c.* 400–300 cal. yr BP). The early Holocene was a well-defined calm period.

Four pronounced pre-historic flooding periods occurred approximately *c.* 6900–6000, 4300–3000, 1700–1300 and the recent 800 cal. yr BP. A previous study of lake Butjønna (Drange, 2002) confirms that the uppermost 25 river floods identified in the sedimentological archive tie in nicely with the equivalent study from the adjacent and significantly larger catchment of the river Atna (Nesje *et al.*, 2001a). These results are thus regarded as valid on a regional scale. High-frequency, minor river floods seem to have occurred during warmer periods. Fewer, but larger floods occurred apparently during cold periods (Drange, 2002). It is likely that the latest period of enhanced flood frequency reflects the 'Little Ice Age' (LIA), AD 1350–1920). Lower air temperatures, thicker and longer-lasting snow cover in addition to increased storm frequency characterized the LIA (eg, Grove, 2001; McCarroll *et al.*, 2001; Nesje and Dahl, 2003).

Flood recurrence interval and probability

The recurrence interval (T) and occurrence probability (P) are inversely proportional; $T = 1/P$. T_1 (Table 2) is the empirical mean of about 90 years with a corresponding occurrence probability, $P_1 = 0.0116$. Subsequently, there is an about 1% chance each year that the Butjønna catchment will experience erosional flooding. T_2, T_3 and T_4 (Table 2), calculated by various plotting equations, consider different extreme value distributions, but take no account of the exact dependence on flood sediment thickness. The variance between T_2, T_3 and T_4 is essentially small, except from the estimates for thickness classes with only one flood as a statistical basis. The equations for T_2, T_3 and T_4 are based on statistically derived relationships from shorter timescales and no real knowledge of the actual occurrences of floods (Cunane, 1978). Further spectral analyses to detect links to external periodicities are not emphasized in this study because of the concerns about the non-stationary signal and the small statistical number.

Comparison with regional climate parameters

This prehistoric river flood record shows an independent terrestrial record of increasing extreme weather events. Lake Butjønna experiences a high discharge rate because of spring melting of snow. Enhanced winter precipitation is a possible consequence of more insolation energy in wintertime, considering the capacity of warm air to contain more humidity. Southern Norway is dominated by prevailing southwesterly wind fields. The moist air enters the circulating air masses across the relatively warm sea, and is released as orographic exaggerated frontal precipitation. East-central southern Norway, however, is in the rain shadow for the prevailing southwesterly wind fields, but the plateau Glacier Hardangerjøkulen lies on the central east–west watershed. The reconstructed winter precipitation from glacier fluctuations and independent summer temperatures demonstrates a clear declining trend in magnitude, but increased oscillation with smaller amplitudes throughout Holocene (Dahl and Nesje, 1994, 1996). The early Holocene shows several periods of winter precipitation as high as about 200% above present values (Figure 7). Hence, an apparent shift from a southwesterly wind-dominated precipitation pattern occurred during the mid-Holocene (*c.* 7000–6000 cal. yr BP). Variations of the Glaciers Hardangerjøkulen (Dahl and Nesje, 1994, 1996) and Jostedalsbreen (Nesje *et al.*, 2001b) confirm less glacier accumulation after mid-Holocene. The Lake Butjønna flood archive possibly reflects the position of the wind fields providing precipitation in eastern Norway, contrary to the amount of winter precipitation in western Norway. Phases of higher lake level in mid-Europe (Magny *et al.*, 2003) coincide with glacier maximums in the Swiss Alps (Holzhauser *et al.*, 2005), and are apparently anti-phased with high flood frequency in east-central southern Norway.

Studies of extreme weather events from western Norway jointly indicate a regional increase in slope-wasting processes, with an onset *c.* 3200 cal. yr BP (eg, Matthews *et al.*, 1986, 1997; Nesje *et al.*, 1991, 1994; Blikra and Nemec, 1993, 1998). Intensified rainstorms lead to increase in debris-flow processes from *c.* 2200 cal. yr BP (Sletten *et al.*, 2003) (Figure 7).

There is an observed relationship between European flood events and large-scale atmospheric circulation (Uvo, 2003; Jacobeit *et al.*, 2003). By decomposing prevailing wind fields in two elements, southerly and westerly flow, it may be possible to link terrestrial climate archives to variations in one of these two contributing airflows. Periods of enhanced southerly winds, bringing moist air from the Atlantic Ocean, correspond with high flooding frequency (Øyvind Lie, personal communication,

2005). The atmospheric data demonstrate a clear correspondence between weakened southerly wind fields and the absence of flooding in Lake Butjønna. From all the mentioned records, extreme weather events seem to increase during the late Holocene. Seen on a larger scale, the periods of extreme weather events east and west of the Norwegian watershed do not seem to coincide to a more detailed extent. Increased southerly or westerly winds lead to flooding activity in eastern Norway, and slope-wasting processes in western Norway, respectively.

Summary and conclusions

(1) The question of possible escalation in magnitude and number of extreme weather events through time in southern Norway has been addressed using a natural sediment trap in a small basin. The implications of this lacustrine sedimentological lithostratigraphy is a palaeoflood record of about 115 Holocene river floods. These discrete flood layers are 1–620 mm thick and exhibit sharp, but non-erosional contacts with both underlying and overlying gyttja. The flood layers consist of silt and clay and are in most cases fining upwards.

(2) An energy-measure in this flood layer reconstruction is based on the negative correlation between the mean grain-size and sorting parameters. The mean grain-size values increase with flood layer thickness. The sorting parameter shows an equivalent negative trend ($2.3–2.9\sigma_g$).

(3) The age–depth model is based on 13 stratigraphically consistent ^{14}C AMS dates on terrestrial plant macrofossils with standard deviations of 25–50 years. A coupled age–depth model was calculated based on a linear regression model after subtraction of the flood layers. The mean sedimentation rate was 0.48 mm/yr, which implies a general time resolution of ~ 2 yr/cm.

(4) Magnetic measurements are for the first time applied to a Holocene river flood record. Down-core magnetic variations show a weak χbulk susceptibility signal in the order of $0–2 \times 10^{-8}$ m^3/kg. Intervals and episodes showing relatively high concentrations of magnetic minerals are equivalent to the minerogenic flood layers. The magnetic measurements suggest an early Holocene calm period, where the depositional regime hardly experiences any river floods.

(5) A megaflood is described and correlated to the major eighteenth century flood disaster 'Stor-Ofsen' in July AD 1789. Better sorted sediments and an increased proportion of very coarse silt indicate three episodes of flood intensification. High χbulk susceptibility values reflect continuous high minerogenic inputs of larger (MD) magnetic grains. A possible import of foreign magnetic particles from the nearby regional river Grimsa is suggested during the culmination of 'Stor-Ofsen', because of extreme σSIRM values and occurrence of MD grains > 10 μm.

(6) Four pronounced prehistoric flooding periods are recognized *c.* 6900–6000, 4300–3000, 1700–1300 and the recent 800 cal. yr BP. The flood frequency indicates a weak growing (parabolic shaped) trend throughout the Holocene, and varies from zero (early Holocene) to seven (*c.* 400–300 cal. yr BP) floods per 100-yr interval. The latest period of enhanced flood frequency happened during the 'Little Ice Age' (*c.* 650–100 cal. yr BP).

(7) Lake Butjønna experiences a recurrence interval of about 90 years, subsequently with a corresponding occurrence probability of about 1%. According to flood thickness, other estimates are calculated by various plotting equations based on the assumption of extreme value distributions. These statistically derived relationships give comparable results, but are constrained by the non-stationarity within the data.

(8) Lake Butjønna flood archive possibly reflects the position of the wind fields providing precipitation in eastern Norway, contrary to the winter precipitation amounts in western Norway. Periods with dominance of southerly winds, bringing moist air from the Atlantic Ocean, correspond with high flood frequency. Increased southerly or westerly winds lead to flooding activity in eastern Norway, and slope-wasting processes in western Norway, respectively.

Acknowledgements

Lars Ivar Folgerø, Herbjørn Heggen and Henriette Linge assisted with the lake coring. The mineral magnetic measurements were carried out in Reidar Løvlie's laboratory at the University of Bergen. The authors appreciate enviromagnetic discussions with Øyvind Paasche and Reidar Løvlie, and are grateful to Anne Bjune for guidance in identifying macrofossils. This work is in corroboration with NORPEC, a NFR-funded Strategic University Program (SUP) headed by Professor H.J.B. Birks. This is publication No. A 85 from the Bjerknes Centre for Climate Research.

Appendix 1

M	Volume magnetization	A/m
δ	Density	kg/m^3
σ	Mass magnetization	Am^2/kg
κ	Volume susceptibility	–
χ	Mass susceptibility	M^3/kg
$K = \kappa \times$ volume	Bulk susceptibility	M^3
$\chi = \kappa/\delta$	Mass spesific magnetic susceptibility	m^3/kg
MS	Magnetic susceptibility (P)	m^3/kg
-0.9×10^{-8}	Water correction	m^3/kg
ARM	Anhysteretic remanent magnetization: aquired by the decay of an assymetric alternating field (af) from a peak value to zero	A/m^2 per kg or A/m
SIRM	(Saturation) Isothermal remanent magnetization: aquired by imposing a certain DC field to a sample at at constant temperature, indication of large MD magnetic grains > 10 μm	A/m
$S_{0.1T}$	S-ratio of the IRM from a backfield at the level of 0.1T in a positive field of 3T. The ratio serves to discriminate magnetite from hematite. Concentration independent	–
ARM/SIRM	Granolumetric variations	–
ARM/MS	Granolumetric variations	–

References

Arnaud, F., Lignier, V., Revel, M., Desmet, M., Beck, C., Pourchet, M., Charlet, F., Trentesaux, A. and **Tribovillard, N.** 2002: Flood and earthquake disturbance of Pb-210 geochronology (Lake Anterne, NW Alps). *Terra Nova* 14, 225–32.

Bakke, J., Dahl, S.O., Paasche, Ø., Løvlie, R. and **Nesje, A.** 2005: Glacier fluctuations, equilibrium-line altitudes and palaeoclimate in Lyngen, northern Norway, during the Lateglacial and Holocene. *The Holocene* 15, 518–40.

Benito, G. 2003: Paleoflood hydrology in Europe. In Thorndycraft, V.R., Benito, G., Barriendos, M. and Llasat, M.C., editors, *Paleofloods, historical data & climatic variability: applications in flood risk assessment*. Proceedings of the Palaeofloods, Historical Floods and Climatic Variability: Applications in Flood Risk Assessment International Workshop, 2002.

Blikra, L.H. and **Fjellstad Selvik, S.** 1998: Climatic signals recorded in snow avalanche-dominated colluvium in western Norway: depositional facies successions and pollen records. *The Holocene* 8, 631–58.

Blikra, L.H. and **Nemec, W.** 1993: Postglacial avalanche activity in western Norway: depositional facies sequences, chronostratigraphy and paleoclimatic implications, In Frenzel, B., Matthews, J.A. and Gläser, B., editors, Solifluction and climate variation in the Holocene. *Paläoklimaforchung* 11, 143–62.

—— 1998: Postglacial colluvium in western Norway: depositional processes, facies and paleoclimatic record. *Sedimentology* 45, 909–45.

Blikra, L.H. and **Nesje, A.** 1997: Holocene avalanche activity in western Norway: chronostratigraphy and palaeoclimatic implications. *Paläoforschung* 19, 299–312.

Bogen, J. 1983: *Atnas delta i Atnsjøen: en fluvialgeomorfologisk undersøkelse.* Rapport Kontaktutvalget for vassdragsreguleringer, University of Oslo (in Norwegian).

—— 1989: *Forsknings- og referansevassdrag Atna: transport av suspendert materiale og substratforhold i Atnavassdraget.* MVU-rapport B 52, NTNF's utvalg for miljøvirkninger av vassdra gsutbygging (in Norwegian).

—— 2004: Erosion and sediment yield in the Atna river basin. *Hydrobiologica* 521, 35–47.

Bogen, J. and **Bønsnes, T.E.** 1999: *Miljøvirkninger av erosjon og sedimenttransport under flommer.* Hydra-rapport Nr. 5, The Norwegian Water and Resources and Energy Directorate (NVE) (in Norwegian).

Bond, G., Showers, W., Cheseby, M., Lotti, R., Almasi, P., deMenocal, P., Priore, P., Cullen, H., Hajdas, I. and **Bonani, G.** 1997: A pervasive millennial-scale cycle in North Atlantic Holocene and glacial climates. *Science* 278, 1257–66.

Brazdil, R., Glaser, R., Pfister, C. and **Stangl, H.** 2002: Floods in Europe – a look into the past. *Science Highlights Pages News* 10.

Briffa, K.R., Osborn, T.J. and **Schweingruber, F.H.** 2004: Large-scale temperature inferences from tree rings: a review. *Global and Planetary Change* 40, 1–2.

Bronstert, A. 2003: Floods and climate change: interactions and impacts. *Risk Analysis* 23, 545–57.

Brown, S.L., Bierman, P.R., Lini, A. and **Southon, J.** 2000: 10 000 yr record of extreme hydrologic events. *Geology* 28, 335–38.

Christensen, J.H. and **Christensen, O.B.** 2002: Severe summertime flooding in Europe. *Nature* 421, 805.

Cunane, C. 1978: Unbiased plotting positions – a review. *Journal of Hydrology* 37, 205–22.

Dahl, S.O. and **Nesje, A.** 1994: Holocene glacier fluctuations at Hardangerjøkulen, central-southern Norway: a high-resolution composite chronology from lacustrine and terrestrial deposits. *The Holocene* 4, 269–77.

—— 1996: A new approach to calculating Holocene winter precipitation by combining glacier equilibrium-line altitudes and pine-tree limits: a case study from Hardangerjokulen, central southern Norway. *The Holocene* 6, 381–98.

Dahl, S.O., Bakke, J., Lie, O. and **Nesje, A.** 2003: Reconstruction of former glacier equilibrium-line altitudes based on proglacial sites: an evaluation of approaches and selection of sites. *Quaternary Science Reviews* 22, 275–87.

Det Norske Meteorologiske Institutt – Klimaavdelingen (DNMI) 1993: *Temperatur – og nedbørs-normaler 1961–1990.* DNMI.

Drange, E.M. 2002: Et paleohydrologisk studie av Sagbekken, Hedmark fylke: En rekonstruksjon av Sagbekkens flomhistorie gjennom holosen. Master Thesis in physical geography, Department of Geography, University of Bergen (in Norwegian).

Evans, M.E. and **Heller, F.** 2001: Magnetism of loess/palaeosol sequences: recent developments. *Earth-Science Reviews* 54, 129–44.

Grove, J.M. 2001: The initiation of the 'Little Ice Age' in regions round the North Atlantic. *Climate Change* 48, 53–82.

Gunn, D.E. and **Best A.I.** 1998: A new automated nondestructive system for high resolution multi-sensor core logging of open sediment cores. *Geo-Marine Letters* 18, 70–77.

Holzhauser, H., Magny, M. and **Zumbühl, H.J.** 2005: Glacier and lake-level variations in west-central Europe over the last 3500 years. *The Holocene* 15, 789–801.

Jacobeit, J., Glaser, R., Luterbacher, J., Nonnenmacher, M. and **Wanner, H.** 2003: Links between flood events in central Europe since AD 1500 and the large-scale atmospheric circulation. In Thorndycraft, V.R., Benito, G., Barriendos, M. and Llasat, M.C., editors, *Paleofloods, historical data & climatic variability: applications in flood risk assessment.* Proceedings of the Palaeofloods, Historical Floods and Climatic Variability: Applications in Flood Risk Assessment International Workshop, 2002.

Knox, J.C. 2000: Sensitivity of modern and Holocene floods to climate change. *Quaternary Science Reviews* 19, 439–57.

Lins, H.F. and **Cohn, T.A.** 2003: Floods in the greenhouse: spinning the right tale. In Thorndycraft, V.R., Benito, G., Barriendos, M. and Llasat, M.C., editors, *Paleofloods, historical data & climatic variability: applications in flood risk assessment.* Proceedings of the Palaeofloods, Historical Floods and Climatic Variability: Applications in Flood Risk Assessment International Workshop, 2002.

Macklin, M.G. and **Lewin, J.** 2003: River sediments, great floods and centennial-scale Holocene climate change. *Journal of Quaternary Science* 18, 101–105.

Magny, M., Bégeot, C., Guiot, J. and **Peyron, O.** 2003: Contrasting patterns of hydrological changes in Europe in response to Holocene climate cooling phases. *Quaternary Science Reviews* 22, 1589–96.

Matthews, J.A., Harris, C. and **Ballantyne, C.K.** 1986: Studies on a gelifluction lobe, Jotunheimen, Norway: ^{14}C chronology, stratigraphy, sedimentology and palaeoenvironment. *Geografiska Annaler* 68A, 345–60.

Matthews, J.A., Dahl, S.O., Berrisford, M.S., Nesje, A., Dresser, P.Q. and **Dumayne-Peaty, L.** 1997: A preliminary history of Holocene colluvial (debris-flow) activity, Leirdalen, Jotunheimen, Norway. *Journal of Quaternary Science* 12, 117–29.

McCarroll, D., Shakesby, R.A. and **Matthews, J.A.** 2001: Enhanced rockfall activity during the Little Ice Age: further lichenometric evidence from a Norwegian talus. *Permafrost and Periglacial Processes* 12, 157–64.

Milly, P.C.D., Wetherald, R.T., Dunne, K.A. and **Delworth, T.L.** 2002: Increasing risk of great floods in a changing climate. *Nature* 415, 514–17.

Mudelsee, M., Borngen, M., Tetzlaff, G. and **Grunewald, U.** 2003: No upward trends in the occurrence of extreme floods in central Europe. *Nature* 425, 166–69.

Nesje, A. 1992: A piston corer for lacustrine and marine sediments. *Arctic and Alpine Research* 24, 221–27.

Nesje, A. and **Dahl, S.O.** 2003: The 'Little Ice Age' – only temperature? *The Holocene* 13, 139–45.

Nesje, A., Kvamme, M., Rye, N. and **Løvlie, R.** 1991: Holocene glacial and climate history of the Jostedalsbreen region, western Norway; evidence from lake sediments and terrestrial deposits. *Quaternary Science Reviews* 10, 87–114.

Nesje, A., Aa, A.R., Kvamme, M. and **Sonstegaard, E.** 1994: A record of late Holocene avalanche activity in Frudalen,

Sogndalsdalen, Western Norway. *Norsk Geologisk Tidsskrift* 74, 71–76.

Nesje, A., Dahl, S.O., Matthews, J.A. and **Berrisford, M.S.** 2001a: A c. 4500-yr record of river floods obtained from a sediment core in Lake Atnsjøen, eastern Norway. *Journal of Paleolimnology* 25, 329–42.

Nesje, A., Matthews, J.A., Dahl, S.O., Berrisford, M.S. and **Andersson, C.** 2001b: Holocene glacier fluctuations of Flatebreen and winter-precipitation changes in the Jostedalsbreen region, western Norway, based on glaciolacustrine sediment records. *The Holocene* 11, 267–80.

Norges Offentlige Utredninger (NOU), 1996: *Tiltak mot flom.* Norges offentlige utredninger 1996: 16, 207 pp. (in Norwegian).

Østmoe, A. 1985: Storofsen. *Oversiktsregisteret,* Infotrykk, Ski (in Norwegian).

Paasche, Ø., Løvlie, R., Dahl, S.O., Bakke, J. and **Nesje, A.** 2004: Bacterial magnetite in lake sediments: late glacial to Holocene climate and sedimentary changes in northern Norway. *Earth and Planetary Science Letters* 223, 319–33.

Roald, L.A. 1999: *Analyse av lange flomserier.* Hydra-rapport F, F01, Norges vassdrags- og energidirektorat (NVE) (in Norwegian).

—— 2003: Two major 18th century flood disasters in Norway. In Thorndycraft, V.R., Benito, G., Barriendos, M. and Llasat, M.C., editors, *Paleofloods, historical data & climatic variability: applications in flood risk assessment.* Proceedings of the Palaeofloods, Historical Floods and Climatic Variability: Applications in Flood Risk Assessment International Workshop, 2002.

Seierstad, J., Nesje, A., Dahl, S.O. and **Simonsen, J.R.** 2002: Holocene glacier fluctuations of Grovabreen and Holocene snow-avalanche activity reconstructed from lake sediments in Groningstolsvatnet, western Norway. *The Holocene* 12, 211–22.

Seppä, H. and **Birks, H.J.B.** 2001: July mean temperature and annual precipitation trends during the Holocene in the Fennoscandian tree-line area: pollen-based climate reconstructions. *The Holocene* 11, 527–39.

Sletten, K., Blikra, L.H., Ballantyne, C.K., Nesje, A. and **Dahl, S.O.** 2003: Holocene debris flows recognized in a lacustrine sedimentary succession: sedimentology, chronostratigraphy and cause of triggering. *The Holocene* 13, 907–20.

Sollid, J.L. and **Carlsson, A.B.** 1979: *Folldal kvartærgeologisk kart 1:50 000 1519II.* Geografisk Institutt, Universitetet i Oslo.

Sommerfeldt, W. 1943: Ofsen i 1789 og dens virkninger i Kvam. Master Thesis in Geography, University of Oslo, Fron historielag, 1972 (in Norwegian).

Starkel, L. 2002: Change in the frequency of extreme events as the indicator of climatic change in the Holocene (in fluvial systems). *Quaternary International* 91, 25–32.

Stuiver, M., Reimer, P.J., Bard, E., Beck, J.W., Burr, G.S., Hughen, K.A., Kromer, B., McCormac, G., Van der Plicht, J. and **Spurk, M.** 1998: INTCAL98 radiocarbon age calibration, 24,000–0 cal BP. *Radiocarbon* 40, 1041–83.

Thorndycraft, V., Hu, Y., Oldfield, F., Crooks, P.R.J. and **Appleby, P.G.** 1998: Individual flood events detected in the recent sediments of the Petit Lac d'Annecy, eastern France. *The Holocene* 8, 741–46.

Thorndycraft, V.R., Benito, G., Barriendos, M. and **Llasat, M.C.,** editors 2003: *Paleofloods, historical data & climatic variability: applications in flood risk assessment.* Proceedings of the Palaeofloods, Historical Floods and Climatic Variability: Applications in Flood Risk Assessment International Workshop, 2002.

Tvede, A.M. 2004: Hydrology of Lake Atnsjoen and River Atna. *Hydrobiologica* 521, 21–34.

Uvo, C.B. 2003: Analysis and regionalization of northern European winter precipitation based on its relationship with the North Atlantic oscillation. *International Journal of Climatology* 23, 1185–94.

Walden, J., Slattery, M.C. and **Burt, T.P.** 1997: Use of mineral magnetic measurements to fingerprint suspended sediment sources: approaches and techniques for data analysis. *Journal of Hydrology* 202, 353–72.